A Semi-Automatic Method for Segmentation of the Coronary Artery Tree from Angiography

Daniel S.D. Lara and Alexandre W.C. Faria and Arnaldo A. de Albuquerque
Computer Science Departament
UFMG - Belo Horizonte (MG) - Brazil
Email: {daniels,awcfaria,arnaldo}@dcc.ufmg.br

David Menotti
Computer Science Department
UFOP - Ouro Preto (MG) - Brazil
Email: menottid@gmail.com

Abstract—Nowadays, medical diagnostics using images has a considerable importance in many areas of medicine. It promotes and makes easier the acquisition, transmission and analysis of medical images. The use of digital images for diseases evaluations or diagnostics is still growing up and new application modalities are always appearing. This paper presents a methodology for a semi-automatic segmentation of the coronary artery tree in 2D X-Ray angiographies. It combines a region growing algorithm and a differential geometry approach. The proposed segmentation method identifies about 90% of the main coronary artery tree.

Keywords-Image Segmentation; Coronary Artery Tree; Angiography;

I. Introduction

Blood vessels detection is an important step in many medical application tasks, such as automatic detection of vessel malformations, quantitative coronary analysis (QCA), vessel centerline extractions, etc. Vessel detection is a recognition problem that is challenging due to the complex nature of vascular trees and to imaging imperfections [1]. Blood vessel segmentation algorithms are the key components of automated radiological diagnostic systems [2]. A wide variety of automatic blood vessel segmentation methods have been proposed in the last two decades. These methods used approaches that varied from Pattern Recognition techniques [3]–[11], Model-based Approaches [12]–[18], Tracking-Based Approaches [19]–[22], Artificial Intelligence Approaches [23]–[26] until Neural Network-based approaches [27]–[29]. In [2], Kirbas and Queek presented a well referenced survey of some of those vessel segmentations methods.

Even with all these efforts, only few of these methods achieved enough results to be applied in a system allowing the user to give a minimum input. The major part of them has too many parameters to be adjusted depending on the image quality. Once these parameters are all set, the user does not need to change anything for similar quality images. However, the nature of X-Ray angiograms leads to a possible low or high contrast images depending on the patient weight. It means that even if all the segmentation algorithm parameters, X-Ray Generator dose, Camera adjustments and image intensifier fields are the same, the image quality can vary depending on the patient weight.

O'Brien and N. Ezquerra [30] proposed a region growing method for coronary (cardiac arteries) segmentation that did not need successive user refinements. This method took a rectangular local region around the coronary intending to realize local searches in order to detect the vessel. The process was performed in many temporal acquired frames (Cine frames) to avoid problems caused by intodisjoint segments. Intodisjoint segments could be caused by noise, image artifacts, structural defects (*e.g.*, a stenosis), etc. The main disadvantage of this approach resides on the fact that it needs to search vessels in other sequential frames to eliminate any other user-supplied seed points. It makes the final result dependent on the possibility of next frames appearing without the same discontinuities identified before. Supposing, for example, the discontinuity is a stenosis, it will be present in many sequential frames stopping the region to grow anyways.

Schrijver [7] proposed a multi-scale coronary tree segmentation based on a differential geometry approach. Basically, it processes the angiogram with a multi-scale vessel detector, applies a vessel resemblance function, allows the user to change some parameters to reach the best results and traces the arteries. As explained before, this method also requires a lot of parameters to automatically obtain great results for each angiogram. However the vessel resemblance function proposed by [7] could be an excellent seed generator for a region growing method.

In this paper, we present a hybrid region growing method with a differential geometry vessel detector for coronary segmentation. It intends to reach the advantages from both and tries to avoid at most the user parameter adjustments. Figure 1 shows an overview of the method.

This paper is organized as follows. Section II describes the segmentation method, where Section II-A explains in details the region growing step, Sections II-B and II-C explain the Hessian and vessel resemblance function, and Section II-D presents the algorithm for the whole segmentation process. Analysis of results of our method is presented in Section III, whilst conclusions and future works are pointed out in
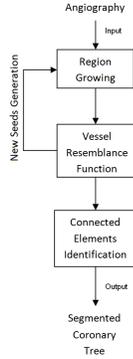
Figure 1. Method overview

Section IV.

II. OUR SEGMENTATION METHOD

A common problem in methods based in only region growing is their difficulty to continue growing up the segmented area if any artifact or vessel blockage (*e.g.*, stenosis) drives the region to a minimum area to be segmented (discontinuities). Usually these methods must find a way to overpass this challenge. Aiming to avoid these non desired characteristics, this proposal starts with a region growing followed by a differential geometry vessel detector. The last is not intended to segment the vessels at all, it is suggested to generate new seeds for those possible vessels branches which were not identified by the first. The next subsections will explain each step in details.

A. Region Growing

Although human beings can easily segment angiograms, this is not an easy task to be implemented in a computational environment. Some image artifacts as bones or muscle tissues can be presented in X-Ray angiograms as vessel like structures (Tubular). These structures can be misunderstood by a global coronary segmentation search as being a vessel. It means that a local search could be a good starting option for coronary segmentations. Furthermore, more sophisticated solutions (which can include global searches) can be incorporated to the initial local search to refine the results. Therefore, the region growing step proposed here starts with a first vessel point given by a user mouse click. O'Brien and N. Ezquerra [30] formalized part of this idea as the following:

Once an initial point, $S_0 = (x, y)$ which lies somewhere on the vessel structure is available, a search will be performed. Thus, the following assumptions are used:

1) The area which is part of the vessels is required to be "slightly darker" than the background;
2) For some sample area in the image, such as a circle window, if the area is large enough, the ratio of vessel area to background area, say a_v/a_b, will be less than some constant C and greater than other constant D for each image;
3) The vessel segments are "elongated" structures;
4) The width of a healthy (non-stenotic) blood vessel changes "slow";
5) The pixel values change "slowly" along with the length of the connected vessels except where some object may intersect or occlude the blood vessel (*e.g.*, overlapping bifurcations).

In this way, starting with an initial seed $S_0(x, y)$, the method defines a circle centered in S_0 with radius r_0. Niblack thresholding [31, pages 115-116] is used to identify two classes of pixels in the circle. Let t be the Niblack threshold for a circle c. Those pixels in c darker than t are supposed to be vessel points. Pixels in c brighter than t constitute the background. Then, the vessel diameter d_0 at the circle extremity can be identified. Once d_0 is found, its mean point becomes a new seed S_1. A new circle with radius d_0 centered in S_1 is traced and the segmentation process starts again. This recursive step is then repeated until the diameter d_n reaches a minimum value m. Figure 2 shows the above idea.
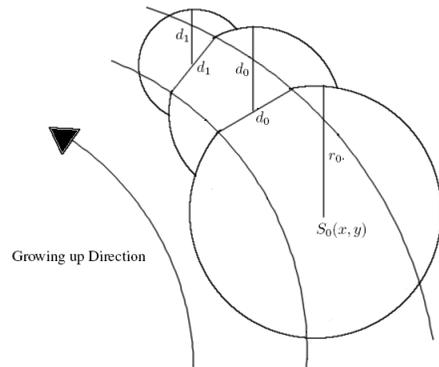

Figure 2. Region growing algorithm

B. Vessel Resemblance Function

The step followed by the region growing is the Vessel Resemblance Function computation. This function proposed by [7] assigns vessel resemblance values for each pixel of the angiography. In order to define this Vessel Resemblance Function, let the angiography $g(u, v)$ be seen as a three-dimensional surface as:

$$G = \{(u, v, z) | z = g(u, v)\}, \quad (1)$$

where u and v extends over the support of $g(u, v)$. Then, for all grid point $x = (u, v)$, the surface curvature is described by the Hessian matrix $H(x)$:

$$H(x) = \begin{bmatrix} g_{uu}(x) & g_{uv}(x) \\ g_{vu}(x) & g_{vv}(x) \end{bmatrix}, \quad (2)$$
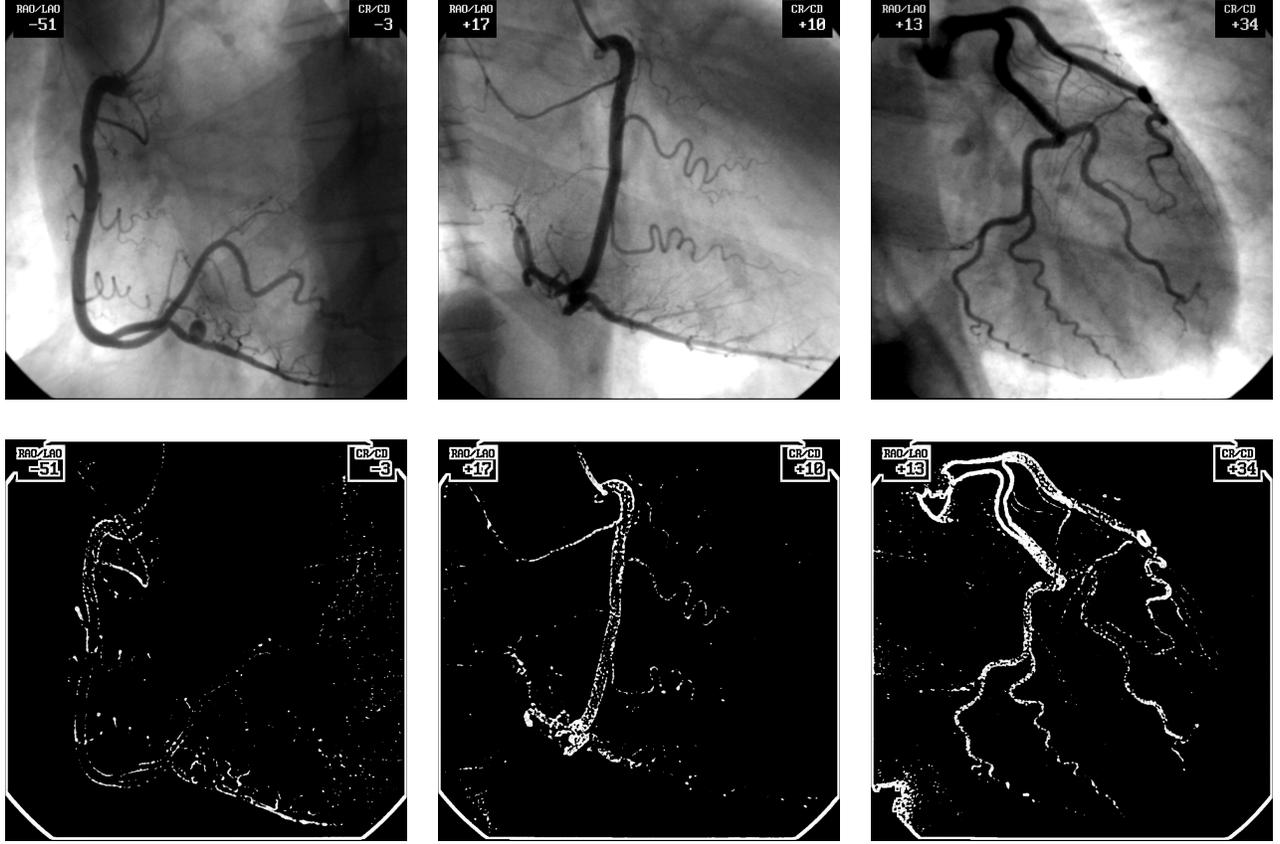
Figure 3. Vessel resemblance function results

where $g_{uu}(x)$, $g_{uv}(x) = g_{vu}(x)$, and $g_{vv}(x)$ are the second-order spatial derivatives of $g(x)$. These derivatives can be calculated by a convolution of a second order spatial derivatives of a Gaussian filter at a scale σ with $g(x)$ ([7], [32], [33] and [34]):

$$g_{ab}(x; \sigma) = \sigma^2 h_{ab}(x; \sigma) * g(x). \qquad (3)$$

From an analysis of the eigenvalues and eigenvectors of the Hessian matrix, it is noticeable that the Hessian matrix strongest eigenvalue and its corresponding eigenvector in a point (u, v) give the 3D-surface strongest curvature and its direction. The eigenvector corresponding to the weaker eigenvalue represents the surface direction perpendicular to the strongest curvature.

As the Hessian matrix is a function of scale σ then the eigenvalues are also. Furthermore λ_i could be written as $\lambda_i(x; \sigma)$. However, supposing we are working with only one scale, and for simplicity, it will be abbreviated by λ_i and its corresponding eigenvector by v_i. For the subsequent analysis, it is supposed the eigenvalues are ordered according to:

$$|\lambda_1| \geq |\lambda_2|. \qquad (4)$$

In this way, assuming an angiography point $x = (u, v)$

being part of a vessel, the eigenvector v_1 is perpendicular to the vessel in x. It happens because the vessels are considered to be a darker region against a brighter background. It means the strongest Hessian eigenvalue is positive in x and the strongest surface curvature is perpendicular to the vessel in x. Furthermore, v_2 will be parallel to the vessel in x. Also, the assumption 3 proposed by [30] allows us to conclude that the weaker Hessian eigenvalue should be small in x. In other words, the surface G has a little curvature on the vessel direction. The following summarizes these characteristics for the vessel point $x = (u, v)$:

$$\lambda_1 > 0 \text{ and } \lambda_2 \approx 0. \qquad (5)$$

Based on all these considerations, the following vessel resemblance function $V(x; \sigma)$, is defined ([32]):

$$V(x; \sigma) = \begin{cases} 0 & \text{if } \lambda_1 < 0 \ , \\ \exp\left(\frac{R_B^2}{2\beta_1^2}\right) \left[1 - \exp\left(\frac{-S^2}{2\beta_2^2}\right)\right] & \text{otherwise} \end{cases}, \qquad (6)$$

where R_B is a measure of how $|\lambda_1|$ is bigger than $|\lambda_2|$, *i.e.*,

$$R_B = \frac{|\lambda_2|}{|\lambda_1|}, \qquad (7)$$

and S is a measure of the strength of the overall curvature:

$$S = \sqrt{\lambda_1^2 + \lambda_2^2}. \qquad (8)$$

The parameters $\beta_1 > 0$ and $\beta_2 > 0$ are scaling factors influencing the sensitivity to R_B and S respectively.

Images in Figure 3 shows an angiography processed by applying the vessel resemblance function. The ones in the first column have resolution of 512×512, whilst the others have 1024×1024 pixels. The parameters used for the image in both rows are the same: $\sigma = 2$, $2\beta_1^2 = 16$ and $2\beta_2^2 = 128$, and they were chosen based on upper and lower bound determinations from [33] *apud* [35].

Next subsection explains how to use these results to obtain region growing seeds automatically.

C. Identifying the Seeds

The Vessel Resemblance Function returns a value for each pixel in the angiography. It determines if this pixel constitutes part of the vessel or not. In images in Figure 3, most part of the non zero pixels belongs to the vessels. All those ones greater than zero are new possible growing seeds. However, some noise or image artifacts can contribute for a small part of background being misunderstood as vessels. In order to eliminate these cases, some statistics are used. Let n and sd be the mean and standard deviation pixel intensity in the area of the circle defined in Section 2.1, respectively. Then defining t as

$$t = \frac{n - sd}{n}, \qquad (9)$$

allows us to distinguish homogeneous from heterogeneous regions. From the assumption 2 [30] proposed in Section 2.1, it is supposed that the circle centered in any artery region will have part of its area being background and another part being vessel. Also, from the assumption 1 proposed in 2.1, the set of pixels intensities in that circle will be more heterogeneous than if it was centered in a background region only. In other words, for circles centered in background regions only the standard deviation sd will be smaller than for circles centered in arteries. It happens because background regions only will not have the "slightly darker" presence of any blood vessel. Therefore t will be closer to the value 1 when the circle area is more homogeneous and further from 1 otherwise.

After the Vessel Detector Phase, a filtering on the possible seed candidates is done to identify points in the background area. This filtering scans all the pixels greater than zero, traces a circle with radius r_0 centered in each candidate and computes t. Those cases where t is greater than a threshold mean the region is homogeneous (background) and these seeds are discarded.

This process results in a final image with all pixels greater than zero in vessels region. This enhanced image with some vessels points detected will be used for a new region growing step explained in the next subsection.

D. The Segmentation Process

The method was implemented in MatLab and the segmentation process is explained by the following algorithm.

1) The user gives the first vessel point s_0.
2) The step described in Section II-A starts.
3) The step described in Section II-B starts.
4) The filtering stage described in Section II-C is performed.
5) For each seed not discarded in Section II-C, perform the region growing described in Section II-A again.

Since it is a recursive algorithm, its complexity will depend on the coronary diameter as well the the number of coronary branches segmented. For instance, taking an angiography A with dimensions $N = m \times n$, it is possible to say that this algortithm execution time will be $O(N)$ for A. It is understood this way because once a pixel is determined to be part of a vessel or not, it will not be processed again.

### E. Connected Elements Identification

By supposing that the segmented coronary will represent the major area of the segmented portion, connected components theory is used to identify the component with the greatest area.

In some exceptional cases, it is possible that in II-C some pixels that do not belong to the artery area become a seed. For those cases, small isolated segmented parts can appear. However it will generate portions of segmented regions disconnected from the main coronary artery tree. Aiming to elimminate these small possible segmented blobs, all connected components are identified, labeled and the one presenting the greatest area is showed as the final coronary artery tree segmented.

III. EXPERIMENTAL RESULTS

In order to evaluate the proposed method, we sampled five Left Coronary Artery (LCA) angiographies and five Right Coronary Artery (RCA) angiographies. Images in Figure 5 are three experimental results. All images are 1024×1024 pixels, 8 bits gray-scale, and they were recorded using a SISMED Digitstar 600N system.

The evaluation of our method is performed as follows. For each image, we manually produce two reference images. The first one with primary arteries (which includes main coronary and first order derivations), and the second with secondary arteries (second order derivations). These arteries are represented by their center lines. Figure 4 illustrates a typical image of a coronary and a representation of its reference images joined. Note that the artery center lines are surrounded by green and purple contours, primary and secondary arteries, respectively. These representations are used for illustrations reasons. From these reference images, it is possible to compute the method accuracy by intersecting the portions between the artery center lines and the resultant segmented arteries.
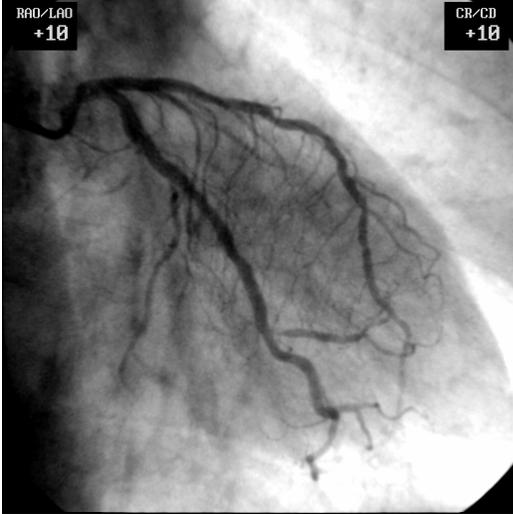
(a) Original Image
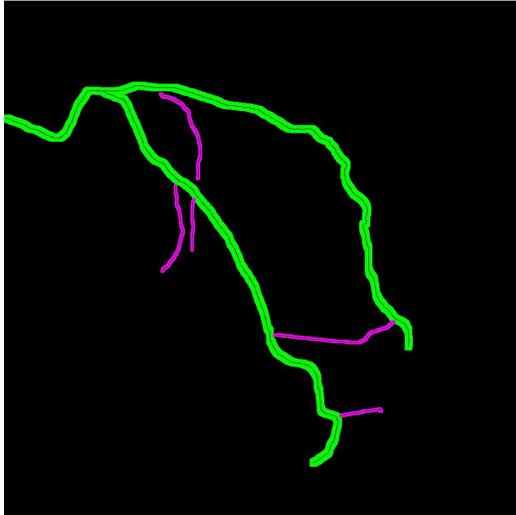
(b) Reference Image

Figure 4. A typical angiography and a union of its reference images

This evaluation in two artery classes is motivated by the nature of the coronary analysis. For instance, in applications where the artery segmentation tree is used, such as quantitative coronary analysis, the task is basically done in main and first order coronaries.

Table I presents the evaluation results for all 10 processed images.

Our method segments the primary coronaries with accuracy of $88.79\% \pm 10,42\%$ ($\mu \pm \sigma$), where the accuracy is defined as described above (the intersection portions between the artery center lines and the resultant segmented arteries). It also segments secondary coronaries with $22.04\% \pm 10.18\%$.

Figure 5 illustrates three samples of our database, where

Table I
IDENTIFICATION OF THE CORONARY ARTERY TREE

Image	Type	Primary	Secondary
01	RCA	96.46%	16.67%
02	RCA	100.00%	35.14%
03	LCA	98.75%	34.01%
04	LCA	63.28%	0.00%
05	RCA	89.60%	24.04%
06	RCA	89.17%	20.97%
07	RCA	83.74%	18.97%
08	LCA	92.01%	28.86%
09	LCA	88.60%	16.40%
10	LCA	86.28%	25.39%
Mean		88.79%	22.04%
Std		10.42%	10.18%

angiographies in the first row are the original images, and its respective segmented coronary artery tree in the second row. Also, for each image in the second row, the arteries are identified by a set of colors. The colors are used to enhance the different regions of the segmented images. The green and red portions represent the non- and segmented primary arteries by the method, respectively. In contrast, the non- and segmented secondary arteries are represented by the purple and blue parts, respectively. It is important to notice that the colored regions only highlight the artery center line identification. In fact, the real thickness (or diameter) of the arteries is unknown.

By observing the images in Figure 5, we can also state that the primary arteries are well segmented, while the secondary artery segmentations still need improvements. This statement agrees with the data presented in Table I.

In spite of the resulting images were not evaluated regarding the segmentation, by observing the images in Figure 5 one can note that, in average, the segmentation is well performed.

IV. CONCLUSION AND FUTURE WORK

A new method for coronary segmentation was presented. Differently from the major part of the methods proposed in literature, this does not need lots of parameter adjustments by the user. Simple ideas were used to contemplate the region growing stage. The results showed that it can be used on a system where the user will have a minimum *a priori* knowledge about the algorithm.

For future works we propose to apply this method in order to automatically detect stenosis by using a hundred more extended database. Also, it was verified that areas of the angiography with a poor contrast make the region difficult to grow. Therefore an interesting characteristic to be added in a pre-processing step is a local vessel contrast enhancement. Furthermore, we propose to evaluate the segmentation accuracy of the proposed method in terms of artery tree area percentage by using reference image, *i.e.*, ground truth image.
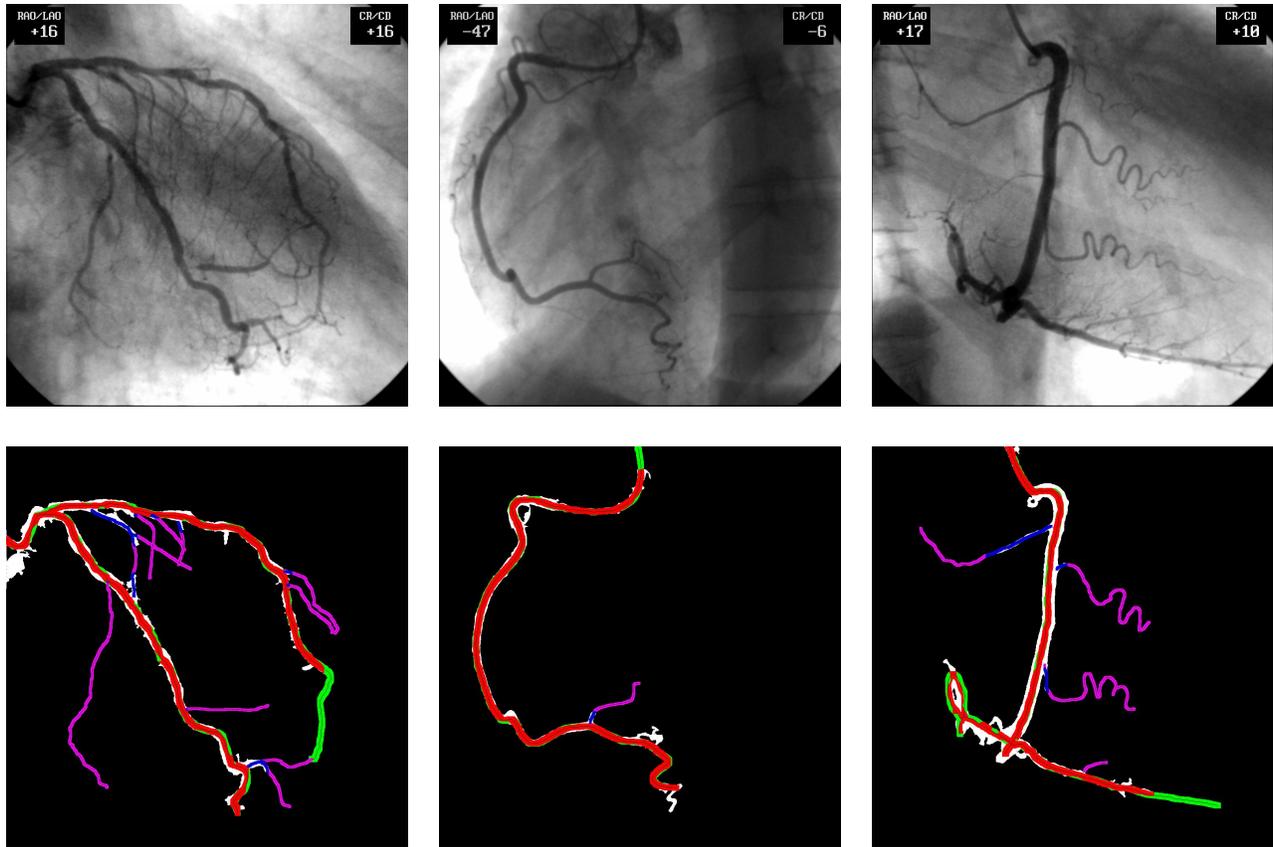
Figure 5. Segmentation results and coronary artery tree identification

REFERENCES

[1] J. Peter, K. Mark, S. Miller, W. Libutti, and P. Choyke, "Automated detection of blood vessels using dynamic programming," *Pattern Recognition Letters*, vol. 24, no. 14, pp. 2471–2478, 2003.

[2] C. Kirbas and F. Quek, "A review of vessel extraction techniques and algorithms," *ACM Computing Surveys*, vol. 36, no. 2, pp. 81–121, 2004.

[3] A. Sarwal and A. Dhawan, "3-d reconstruction of coronary arteries," in *IEEE Conference on Engineering in Medicine and Biology*, vol. 1, 1994, pp. 504–505.

[4] M. Chwialkowski, Y. Ibrahim, F. Hong, and R. Peshock, "A method for fully automated quantitative analysis of arterial flow using flow-sensitized mr images," *Computerized Medical Imaging and Graphics*, vol. 20, no. 5, pp. 365–378, 1996.

[5] E. Sorantin, C. Halmai, B. Erdohelyi, K. Palagyi, L. Nyul, K. Olle, B. Geiger, F. Lindbichler, G. Friedrich, and K. Kiesler, "Spiral-ctbased assessment of tracheal stenoses using 3-d skeletonization," *IEEE Transactions on Medical Imaging*, vol. 21, no. 3, pp. 263–273, 2002.

[6] H. Schmitt, M. Grass, V. Rasche, O. Schramm, S. Haehnel, and K. Sartor, "An x-raybased method for the determination of the contrast agent propagation in 3-d vessel structures," *IEEE Transactions on Medical Imaging*, vol. 21, no. 3, pp. 251–262, 2002.

[7] M. Schrijver, "Angiographic assessment of coronary stenoses: A review of the techniques," *Archives Of Physiology And Biochemistry*, vol. 111, no. 2, pp. 77–158, 2003.

[8] B. J., G. M., and T. C., "Coronary extraction and stenosis quantification in x-ray angiographic imaging," in *IEEE Engineering in Medicine and Biology Society*, vol. 3, 2004, pp. 1714–1717.

[9] Q. Li, J. You, and L. Zhang, "Automated retinal vessel segmentation using multiscale analysis and adaptive thresholding," in *IEEE Southwest Symposium on Image Analysis and Interpretation*, 2006, pp. 139–143.

[10] X. Y., H. Zhang, H. Li, and G. Hu, "An improved algorithm for vessel centerline tracking in coronary angiograms," *Com-*

puter Methods and Programs in Biomedicine, vol. 88, no. 2, pp. 131–143, 2007.

[11] S. Zhou, J. Yang, W. Chen, and Y. Wang, "New approach to the automatic segmentation of coronary artery in x-ray angiograms," *Sci China Ser F-Inf Sci*, vol. 51, no. 1, pp. 25–39, 2008.

[12] J. Molina, S. G. Ellis, and T. et al, "Percutaneous treatment of left main coronary stenosis," *Circulation*, vol. 98, pp. 1587–1590, 1998.

[13] S. Kozerke, R. Botnar, S. Oyre, M. Scheidegger, E. Pedersen, and P. Boesiger, "Automatic vessel segmentation using active contours in cine phase contrast flow measurements," *Journal of Magnetic Resonance Imaging (JMRI)*, vol. 10, no. 1, pp. 41–51, 1999.

[14] H. Luo, L. Qiang, R. Acharya, and R. Gaborski, "Robust snake model," in *IEEE International Conference on Computer Vision and Pattern Recognition*, vol. 1, 2000, pp. 452–457.

[15] L. Sarry and J. Boire, "Three-dimensional tracking of coronary arteries from biplane angiographic sequences using parametrically deformable models," *IEEE Transactions on Medical Imaging*, vol. 20, no. 12, pp. 1341–1351, 2001.

[16] F. Quek and C. Kirbas, "Vessel extraction in medical images by wave propagation and traceback," *IEEE Transactions on Medical Imaging*, vol. 20, no. 2, pp. 117–131, 2001.

[17] W. Law and A. Chung, "Segmentation of vessels using weighted local variances and an active contour model," in *IEEE Conference on Computer Vision and Pattern Recognition Workshop (CVPRW'06)*, 2006, pp. 83–83.

[18] F. G. Lacoste, C. and I. Magnin, "Coronary tree extraction from x-ray angiograms using marked point processes," in *IEEE International Symposium on Biomedical Imaging (ISBI)*, 2006, pp. 157–160.

[19] S. Aylward, S. Pizer, E. Bullitt, and D. Eberl, "Intensity ridge and widths for tubular object segmentation and description," in *Workshop on Math. Methods in Biomed. Image Analysis*, 1996, pp. 131–138.

[20] Y. Tolias and S. Panas, "A fuzzy vessel tracking algorithm for retinal images based on fuzzy clustering," *IEEE Transactions on Medical Imaging*, vol. 17, pp. 263–273, 1998.

[21] F. Quek, C. Kirbas, and F. Charbel, "Aim: attentionally-based interaction model for the interpretation of vascular angiograph," *IEEE Transactions on Information Technology in Biomedicine*, vol. 3, no. 2, pp. 139–150, 1999.

[22] ——, "Aim: An attentionally-based system for the interpretation of angiography," in *IEEE Medical Imaging and Augmented Reality Conference*, 2001, pp. 168–173.

[23] M. Goldbaum, S. Moezzi, A. Taylor, S. Chatterjee, J. Boyd, E. Hunter, and R. Jain, "Automated diagnosis and image understanding with object extraction, object classification, and inferencing in retinal images," in *IEEE International Conference on Image Processing*, vol. 3, 1996, pp. 695–698.

[24] V. Bombardier, M. Jaluent, A. Bubel, and B. J., "Cooperation of two fuzzy segmentation operators for digital subtracted angiograms analysis," in *IEEE Conference on Fuzzy Systems*, 1997, pp. 1057–1062.

[25] U. Rost, H. Munkel, and C. Liedtke, "A knowledge based system for the configuration of image processing algorithms," in *Fachtagung Informations und Mikrosystem Technik*, 1998, pp. 25–27.

[26] R. Socher, A. Barbu, and D. Comaniciu, "A learning based hierarchical model for vessel segmentation," in *IEEE International Symposium on Biomedical Imaging: From Nano to Macro (ISBI'08)*, Paris, France, May 2008, pp. 1055–1058.

[27] R. Nekovei and Y. Sun, "Back-propagation network and its configuration for blood vessel detection in angiograms," *IEEE Transaction on Neural Networks*, vol. 6, pp. 64–72, 1995.

[28] I. Hunter, J. Soraghan, and T. McDonagh, "Fully automatic left ventricular boundary extraction in echocardiographic images," in *IEEE Computers in Cardiology*, 1995, pp. 741–744.

[29] S. Shiffman, G. D. Rubin, and S. Napel, "Semiautomated editing of computed tomography sections for visualization of vasculature," in *SPIE Medical Imaging Conference*, vol. 2707, 1996, pp. 140–151.

[30] J. O'Brien and N. Ezquerra, "Automated segmentation of coronary vessels in angiographic image sequences utilizing temporal, spatial structural constraints," in *SPIE Conference on Visualization in Biomedical Computing*, 1994, pp. 25–37.

[31] W. Niblack, *An Introduction to Digital Image Processing*. NJ, USA: Prentice Hall,, 1986.

[32] A. F. Frangi, W. J. Niessen, R. M. Hoogeveen, T. van Walsum, and M. A. Viergever, "Model-based quantitation of 3-d magnetic resonance angiographic images," *Medical Imaging, IEEE Transactions on*, vol. 18, no. 10, pp. 946–956, 1999.

[33] Y. Sato, S. Nakajima, N. Shiraga, H. Atsumi, S. Yoshida, T. Koller, G. Gerig, and R. Kikinis, "Three-dimensional multi-scale line filter for segmentation and visualization of curvilinear structures in medical images," *Medical Image Analysis*, vol. 2, no. 2, pp. 143–168, 1998.

[34] F.-v.-d. Heijden, *Image based measurement systems: object recognitionand parameter estimation*. John Wiley & Sons, Ltd., 1994.

[35] M. Schrijver and C. H. Slump, "Automatic segmentation of the coronary artery tree in angiographic projections," in *ProRISC*, Nov. 2002, pp. 449–464.